This pre-print refers to the paper presented in 2019 IEEE Milan PowerTech (Milan, 23-27 June 2019), with DOI:10.1109/PTC.2019.8810421

Optimal Planning and Operation Scheduling of Battery Storage Units in Distribution Systems

[1]

Hamidreza Mirtaheri, Alessandro Bortoletto, Maurizio Fantino
LINKS Foundation
Turin, Italy
name.surname@linksfoundation.com {*name.surname*}*@polito.it*

Andrea Mazza
Department of Energy
Politecnico di Torino
Italy, Turin
andrea.mazza@polito.it

Mousa Marzband
Dep. of Physics and Electrical Engineering
Northumbria University
Newcastle upon Tyne, UK
mousa.marzband@northumbria.ac.uk

Abstract

In the last years, the electricity system has been subject to a paradigm change, due to increasing share of installed renewable energy sources-based power plants. This fact is leading electrical system - which proper operation was however affected by the intermittent nature of renewables - to become more "green". The union of energy chain de-carbonization with service reliability opens new opportunities for storage systems, although their relatively high cost highlighted the importance of optimal decisions in sizing, placing and operation of such systems. For addressing these aspects, appropriate mathematical models and optimization methods are needed: in this paper, a novel and efficient hybrid optimization algorithm is introduced, to solve i) sizing, ii) placement and iii) operation of arbitrary storage systems. This method is then applied to a low voltage grid, to demonstrate the effectiveness of the proposed methodology.

Keywords: smart grid, storage system, optimization, genetic algorithm, constraint programming, siting, sizing, scheduling.

[1]This research received support from the EU project Planet founded from the European Union's Horizon 2020 research and innovation programme under grant agreement No. 773839.

This pre-print refers to the paper presented in 2019 IEEE Milan PowerTech (Milan, 23-27 June 2019), with DOI:10.1109/PTC.2019.8810421

1 Introduction

In the recent years, several International agreements have pushed the move towards complete de-carbonization of the energy systems, which should be essentially based on the larger and major exploitation of the Renewable Energy Sources (RES) potentiality [1]. Storage system sizing and siting alongside their optimal use, makes significant profits [2] regardless of its owner class [3]. Commercial Battery Energy Storage System (BESS) owned by electric Distribution System Operator (DSO), aggregator entity or ancillary service provider is expected to deal with power quality, energy loss in the network, Demand Response (DR) service and/or other services, such as reactive power injection. For this category, optimal placing of the storage within the network becomes a decision key and a game changer to benefit both service provider as well as the end-users. Given huge improvements in prediction models thanks to the breakthroughs made in Artificial Intelligence (AI) field [4], BESS control could be instructed considering in distance of days before or even weeks. Looking at the BESS controller as a black-box, the main inputs of the system can be load consumption, RES generation and energy price table, both for private and commercial usage [5], [6].

There have been huge number of research works around the optimization methods addressing electrical network issues, which can consider only single objective (e.g., only losses [7] or reliability [8]) or multi-objective (e.g., losses and reliability [9]). The metaheuristic algorithms [10], inspired by the natural processes, have been successfully applied to the vast area of those problems and proven high sufficiency in term of search result as well as computation burden. The work [6] uses Ant Colony Optimization (ACO) to find the best schedule for BESS. The authors imitated the *Stigmergy* between ants via *pheromone* as heuristic information, to find the best State-of-Charge (SoC) path throughout the time. They made a comprehensive study over various ACO implementation strategies. In [11] an hybrid approach is introduced using mainly Particle Swarm Optimization (PSO) for the storage scheduling. This optimization method is also used in [12] to address ESS and RES operations. Simulated Annealing (SA) is another popular method that can be adapted to the electrical system optimization problems as well [13] There are several works using Genetic Algorithm (GA), such as [14] that is a comprehensive work on optimal sizing and siting the ESS in the LV grid. Other works shown the scheduling of ESS via GA optimization, such as in [15] to handle peak demand, in [16] to reduce energy cost and in [17] to integrate plug-in EV fleet in the grid.

This paper introduces a novel hybrid optimization algorithm to solve i) sizing, ii) placement and iii) operation of arbitrary storage systems and it is organized as follows: Section 2 presents a brief overview of GA and Constraint Programming (CP), whereas Sections 3 and 4 focus on the applied methodology for battery planning and scheduling, respectively. Section 5

This pre-print refers to the paper presented in 2019 IEEE Milan PowerTech (Milan, 23-27 June 2019), with DOI:10.1109/PTC.2019.8810421

describes the considered case study and the obtained results, while the conclusion are shown in Section 6.

2 Heuristic methods: genetic algorithm and constraint programming

This section aims to show the combined use of GA and CP (Section 2.3) , by firstly introducing the basic concepts for both the methods (Section 2.1 and Section 2.2).

2.1 Genetic Algorithm (GA) Optimization

The optimization based on GA is inspired by natural selection and evolution of species [10]. In this context, the chromosomes (i.e., solutions) are combined together through a genetic operator called *crossover*. The solutions that result the best objective function values have higher probability to be selected for the crossover, so they can pass their characteristics to the next generations (allowing to reach the *global optimum*). Thanks to the application of another operator called *mutation* it is possible to avoid falling into possible local minima.

The evaluation of objective function (called *fitness*) is defined according to the problem features, but the solution feasibility remains an issue, due to application of the genetic operators (i.e., crossover and mutation). In order to handle this issue, one of the most common techniques involves the use of *penalty functions* [18]: if specific solution is not feasible, a penalty factor is added to the fitness function, so that the specific chromosome is penalized and likely fails to be selected in the next generation. Although adding a penalty factor is a simple way of implementation, the model might be misled since problem cannot distinguish the cause that would lead to discard a solution (i.e., the value of fitness or feasibility reason).

2.2 Constraint Programming (CP)

CP has been used as a heuristic optimization algorithm, in which the feasibility of every solution is guaranteed, even though the optimality is not [19]. Setting off each single variable, the local constraints are being propagated until meet the global constraints. This action is called *constraint propagation* that yields a pruned domain (variable range) and is being repeated ending to no-further new decision can be made. The resulting solution may not be the optimal one, but it is *at least feasible*, while respects either local and global constraints. This, based on the available resources (computational effort and time) can be iterated without any information inherited from one attempt to another.

This pre-print refers to the paper presented in 2019 IEEE Milan PowerTech (Milan, 23-27 June 2019), with DOI:10.1109/PTC.2019.8810421

2.3 Hybrid GA plus CP

The problems of optimal planning and operating of BESS in electricity distribution system are non-convex and generally hard to map into convex problems, especially in case of multi-objective optimization formulation. In this paper, the optimization model uses the GA as search engine whereas the CP routine supervises initialization of solutions (initial population), combination (crossover) and random insertion (mutation) of those solutions (chromosomes). As mentioned earlier, the solution algorithm covers two completely different aspects: the planning of BESS (i.e., siting and sizing) which will be explained in Section 3, and the optimal scheduling of BESS, which will be detailed in Section 4.

3 BESS Sizing and Siting

3.1 Objective function and constraints of the problem

The optimization model in a first step discovers the optimal placement options for BESS, by considering a long-term (i.e. yearly) horizon of hourly RES generation and load consumption. The goal consists in alleviating voltage deviation and power losses, as shown in eq.(1):

$$_{x\in\mathbb{S}} f(x, E_x, P_x) = \alpha V_{dev} + \beta P_{loss} \tag{1}$$

where x indicates the installation node and $\mathbb{S}$ is a set of possible nodes where the BESS can be connected to, within a known section of the grid. The set $\mathbb{S}$ is formed by ν elements. The variables E_x and P_x stand for BESS capacity installed in the node x and the corresponding converter nominal power, respectively. In eq.(1), the two variables α and β represent the *weights* used for considering both voltage deviation (V_{dev}) and power losses (P_{loss}) obtained after inserting the BESS in the node x in a unique objective function. In this study, the charging and discharging rates of the battery are identical and the power P_x refers to the entire storage system composed of battery cells and converter installed in the node x. The bidirectional converter and battery cells efficiencies are fixed values and are considered not sensitive with respect to temperature, energy level and flowing power.

The BESS capacity E_x in every node is subject to predefined limits linked to the position of the node x with respect to the slack node, as shown in eq.(2).

$$\text{s.t.} \quad E^{min} \leq E_x \leq \frac{E^{max}}{\sum_{i=0}^{q} a_i l_x^i} \tag{2}$$

The variables E^{min} and E^{max} might be set according to a financial/technical analysis, but for sake of simplicity, in this case study, they are predefined values. In eq.(2) the *distance from slack l* has been introduced. It represents

This pre-print refers to the paper presented in 2019 IEEE Milan PowerTech (Milan, 23-27 June 2019), with DOI:10.1109/PTC.2019.8810421

the layer at which the node x belongs to. The layer referred to the slack bus is equal to 0 and so no BESS can be installed in it (excluding substation). For nodes in layers $l \neq 0$, potential installation capacity limit is lower as they are more remote from the slack bus. The factor l can be retrieved from network incident matrix $\mathbf{L}$, describing the radial network. Finally, the coefficients a_i refer to the q order polynomial formulation (arbitrarily chosen by the user, here $q = 1$) used for determining the maximum boundary value of the BESS capacity E_x. The above formulation bounds in turn P_x value definition as in eq.(3).

$$\kappa_1 E_x \leq |P_x| \leq \kappa_2 E_x \tag{3}$$

The charging/discharging rate of battery cells, in general are characterized with C_{rate} meaning that a battery with $n_C C_{rate}$ and $n_D C_{rate}$ can be at fastest charged in $1/n_C$ and discharged in $1/n_D$ hour, and normally $n_C \leq n_D$. In this study, we extend such terminology for complex BESS where κ ranges are varied regarding specific applications rather than electrochemical properties: for example, in case of a utility BESS used for primary frequency regulation, the response should be fast enough and so may acquire high range of κ, that exceed the identity, meaning that the BESS capacity can be filled up and/or discharged in a fraction of hour, while in case of self-consumption exploitation, these rates are lower than 1 [20].

3.2 GA formulation

3.2.1 Initialization of the population

The GA is based on a population composed of Θ chromosomes, each of them containing Ψ *genes*, as shown in eq.(4).

$$\mathbf{G}^{init}_{(\Theta \times \Psi)} = \quad \left[\bar{\mathbf{x}}, \bar{\mathbf{E}}, \bar{\mathbf{p}}\right]^T \tag{4}$$

It is worth to note that the number of chromosomes Θ can be higher than eligible nodes to install BESS ν. Each chromosome represents a BESS, and in this case study, with $\Psi = 3$, the genes of every chromosome represent the location (i.e., the node x), the capacity of battery E_x and its power P_x, respectively.

G^{init} is created by a CP routine: $\bar{x}$ is a vector containing all eligible nodes at least once, then according to the eq.(2) vector $\bar{E}$ is generated randomly but respecting global constraints, and propagates local constraint for $\bar{p}$ vector according to $n_C C_{rate}$ and $n_D C_{rate}$ coefficients.

For hosting the objective function values, an additional placeholder vector is added to the matrix $\mathbf{G}$, which at the beginning of optimization process is set to the infinity ($\overline{\infty}$), as in eq.(5).

$$\mathbf{G}_{(\Theta \times \Psi + 1)} = [\mathbf{G}^{init} \quad \overline{\infty}] \tag{5}$$

This pre-print refers to the paper presented in 2019 IEEE Milan PowerTech (Milan, 23-27 June 2019), with DOI:10.1109/PTC.2019.8810421

3.2.2 Calculation of the objective function and the fitness

Once the initial population is created, the classic process of search begins, but with additional CP supervision. At the iteration k, each chromosome $\mathbf{G}(\vartheta, 1:\Psi)$, $\vartheta = 1, .., \Theta$ is the input of network model, that allows to calculate the voltages and power losses along all the year after having introduced that particular BESS (which performs charging and discharging through a dumb hysteresis control), as shown in eq.(6).

$$V_{dev,\vartheta}, P_{loss,\vartheta} \leftarrow \text{Model}(\mathbf{G}(\vartheta, 1:\Psi)), \text{ for } \vartheta = 1, ..., \Theta \tag{6}$$

Where V_{dev} and P_{loss} are the input used for calculating the objective function f_ϑ for every chromosome, as in eq 1, and its inverse (the so-called *fitness*) becomes part of the matrix $\mathbf{G}$:

$$\mathbf{G}(\vartheta, M+1) = 1/f_\vartheta = 1/(\alpha V_{dev,\vartheta} + \beta P_{loss,\vartheta}) \tag{7}$$

3.2.3 Genetic operators (selection, crossover and mutation)

A classic biased roulette wheel method, based on the value of fitness, is used for selecting the chromosomes forming a new population, i.e., $\mathbf{G}_{new}$. From the new population, a number n_p of parents are extracting and forming the matrix $\mathbf{\Pi}$, of dimensions $n_p \times \Psi$, by comparing a threshold ρ_C with a random extraction from a uniform distribution function $U([0,1])$: if the number extracted is lower than ρ_C, then that chromosome will be a parent otherwise not. The extraction is repeated for the successive chromosomes with the same logic. At the end of crossover routine, n_p chromosomes will be substituted by the ones obtained through the recombination of parents. On basis of the chosen parents, a new matrix $\mathbf{R}$ contained the recombined chromosomes is defined. Every pair of parents extracted, is cut in one position $c \in 1, .., \Psi$, selected randomly. Every row of the matrix $\mathbf{R}$ is then defined as:

$$\mathbf{R}(h, 1:\Psi) = [\mathbf{\Pi}(h, 1:c) \quad \mathbf{\Pi}(h+1, c+1:\Psi)] \tag{8}$$

$$\mathbf{R}(h+1, 1:\Psi) = [\mathbf{\Pi}(h+1, 1:c) \quad \mathbf{\Pi}(h, c+1:\Psi)] \tag{9}$$

with $h = 2r+1, r \in \mathbb{N}$ representing odd numbers.

After that, the matrix $\mathbf{G}$ is getting updated as $\mathbf{G}_{(\Theta\times\Psi)} \leftarrow \mathbf{G}_{cr}$. If the crossover, by changing the node, affects the BESS's total capacity, by violating eq.(2), a saturation is made for making the configuration feasible. Consequently, this saturation on the energy imposes limits to the nominal power of the connected converter (according to the eq.(3)) as well; The constraints propagate only to the right.

In the mutation step, some points in the matrix $G_{(\Theta\times\Psi)}$ are randomly chosen by extracting, for every gene, a random number which is compared

This pre-print refers to the paper presented in 2019 IEEE Milan PowerTech (Milan, 23-27 June 2019), with DOI:10.1109/PTC.2019.8810421

with a probability of mutation p_m. Also in this case, the boundaries imposed by eq.(2) and eq.(3) rules should be respected, in such a way that the mutation does not create any unfeasible solution.

After mutation, new population is the input for electrical model solver described in eq.(6), and the cycle continues.

3.2.4 Stop criterion

The stop criterion is reached if the standard deviation of the objective function calculated for the last M iterations is lower than a certain threshold ϵ_{err}.

$$\epsilon_{err} = \sqrt{\frac{1}{M}\sum_{i=1}^{M}(\max(\mathbf{f}_i - \bar{\mathbf{f}}))^2} \tag{10}$$

with $\bar{\mathbf{f}}$ indicating the vector containing the mean values of the objective functions in the last M iterations. As a last source for the stopping, it is also imposed a maximum number of iterations.

4 Operation Scheduling

After finding the best position and configuration of the BESS looking long-range horizon (i.e., yearly-based), in a second phase of objective becomes the evaluation of the optimal day-ahead scheduling for the installed BESS. The core of solving problem remains the novel hybrid GA + CP, but the mathematical formulation is different.

The dispatching matrix is composed of three dimensions, i.e., considered time slots (which maximum value is indicated as T_s) , number of BESS considered ($n = 1...N_{BESS}$) and number of feasible solutions considered N. In practice, the method generates a number of charging and discharging profiles during time, by considering different number of BESS installed.

The SoC is the decision variable, since explicitly contains other information: in fact, indicating Δt as the generic time step duration, SoC_k can be described as a function of the states SoC_{k-1} and SoC_{k+1}, complying cells' characteristics and the power converter features, as shown in eq.(11), both for charging and discharging:

$$SoC_{k\mp1} - \eta_b^{(\frac{\Delta SoC}{\Delta t})}\frac{P_{nom}\cdot\Delta t}{E} \leq SoC_k \leq SoC_{k\pm1} + \eta_b^{(\frac{\Delta SoC}{\Delta t})}\frac{P_{nom}\cdot\Delta t}{E} \tag{11}$$

The η_b is a byproduct of two efficiencies, i.e., battery pack and converter, which are still doubled in a charge-discharge back and forth energy flow. On the other hand, degradation matters, especially for battery cells. This is sometimes simplified e.g. in [15] or often neglected e.g. in [16].

This pre-print refers to the paper presented in 2019 IEEE Milan PowerTech (Milan, 23-27 June 2019), with DOI:10.1109/PTC.2019.8810421

In charging status the efficiency term η_b appears in nominator, while in discharging, will pop up in denominator of the above equation. In eq.(11) charging and discharging efficiency are considered identical.

Scheduling process is similar to planning step: a CP routine generates Θ_s feasible solutions (chromosomes) and these solutions undergo to evaluation and evolution process. In this case, chromosomes are composed of T_s genes, each of them representing the SoC level of a BESS in every time step τ of the simulation window. Tensors (i.e., 3D matrices) involved in processes are the lower bound tensor $\mathcal{L}_{(N_{BESS},N,T_s)}$, the upper bound tensor $\mathcal{U}_{(N_{BESS},N,T_s)}$, the slot order tensor $\mathcal{O}_{(N_{BESS},N,T_s)}$ (which initializes the order of time slots to be set) and the SoC tensor $\mathcal{S}_{(N_{BESS},N,T_s)}$. The procedure allows to reduce the space of search of the solutions, thanks to the successive update of the lower and upper bound tensors.

Let's suppose to consider the BESS b ($b \in 1,\ldots,N_{BESS}$) and the time step τ: the chromosome n ($n \in 1,\ldots,N$) is built following sequences in $\mathcal{O}_{(N_{BESS},N,T_s)}$, through a random extraction from a uniform distribution constrained by the upper and lower bound as in eq.(12).

$$\mathcal{S}_{b,n,\tau} \sim U([\mathcal{L}_{b,n,\tau},\mathcal{U}_{b,n,\tau}]) \tag{12}$$

Starting from the time step τ a constraint propagation on the upper bound $\mathcal{U}$ is applied towards right, as shown in eq. 13:

$$\mathcal{U}_{b,n,\tau:T_s} = \eta_b \cdot \Delta SoC^{max} \cdot \mathbf{a_u} + SoC_{b,n,\tau} \tag{13}$$

where ΔSoC^{max} represents the maximum state-of-charge that can be withdrawn/injected in one slot of time. The term $\mathbf{a_u}$ is defined in eq.(14) and is a vector containing all the time slots from τ to T_s:

$$\mathbf{a_u} = \{u \in N|([1, T_s - \tau])\} \tag{14}$$

Likewise, lower bound $\mathcal{L}$ filters the right hand side with the operation in eq. 15;

$$\mathcal{L}_{b,n,\tau:T_s} = SoC_{b,n,\tau} - \frac{\Delta SoC^{max} \cdot \mathbf{a_u}}{\eta_b} \tag{15}$$

The constraint propagation proceeds at the left side with respect to the point τ as in eq.(16).

$$\mathcal{U}_{b,n,1:\tau} = \frac{\mathbf{b_v}^T \cdot \mathbf{J} \cdot \Delta SoC^{max}}{\eta_b} + SoC_{b,n,\tau} \tag{16}$$

The vector $\mathbf{b_v}$ contains all the time slots from one to τ as in eq.(17).

$$\mathbf{b_v} = \{v \in N|([1, \tau])\} \tag{17}$$

$\mathbf{J}$ is the *adversarial matrix* and is defined as in eq.(18).

This pre-print refers to the paper presented in 2019 IEEE Milan PowerTech (Milan, 23-27 June 2019), with DOI:10.1109/PTC.2019.8810421

$$J_{i,j} = \begin{cases} 1, & j = n - i + 1 \\ 0, & j \neq n - i + 1 \end{cases} \tag{18}$$

The same left side propagation occurs for lower bound $\mathcal{L}$, that can be seen in eq.(19).

$$\mathcal{L}_{b,n,1:\tau} \leftarrow SoC_{b,n,\tau} - \eta_b \cdot \mathbf{b_v}^T \cdot \mathbf{J} \cdot \Delta SoC^{max} \tag{19}$$

Finally, $\mathcal{L}$ and $\mathcal{U}$ are saturated between zero and one, by applying eqs. 21 and 20, respectively.

$$\mathcal{L}_{b,n} \leftarrow \mathtt{max}(\mathcal{L}_{b,n}, \vec{0}) \tag{20}$$

$$\mathcal{U}_{b,n} \leftarrow \mathtt{min}(\mathcal{U}_{b,n}, \vec{1}) \tag{21}$$

The initial population, that is a set of feasible BESS SoC, through proposed method covers the search space in a uniform and homogeneous formation, as those chromosomes are set in a random order. An initial population of 100 chromosome, each formed with 24 genes (hours) is depicted in Fig. 3, for two distinct BESS with different κs, or in other word $\frac{p_x}{E_x}$, that is selected based on the specific usage of the battery.

GA search and evolution is being carried out respecting the main steps, starting from solution evaluation, that is, the improvement of electrical quality and service metrics. In the evaluation, each BESS is intended to operate in favor of installation node x: therefore, the node's downstream aggregated profile plus the resulting BESS power becomes the subject of optimization. This is proceed first deriving BESS power through eq.(22).

$$P_x = \eta_b^{(\nabla_t SoC)} \cdot \nabla_t SoC \cdot E_x \tag{22}$$

The fitness functions and then the score columns are calculated regarding the objective(s) formulation, as eq. 7.All process is quite the same as planning routine, with a different tensor of $\mathcal{G}(N_{BESS}, N, T_s)$.

In crossover, recombination (the same as in eq.(8)) occurs with the constraint propagation again, applies filtering to the right side of cross point c for the parent $n+1$ (Π_{n+1}) by the mean of temporary upper and lower bounds ($\mathcal{L}_{temp}$ and $\mathcal{U}_{temp}$) that practically executes the same eqs.(13) to 19, where the τ point becomes crossover point c.

Finally c gets pruned by those $\mathcal{L}_{temp}$, $\mathcal{U}_{temp}$ instead of $\vec{1}$ and $\vec{0}$. The notations are brought in eq. 23.

$$\begin{aligned} \mathcal{G}^n_{cr} &\leftarrow \mathtt{min}(\mathcal{G}^n_{cr}, \mathcal{U}_{temp}) \\ \mathcal{G}^n_{cr} &\leftarrow \mathtt{max}(\mathcal{G}^n_{cr}, \mathcal{L}_{temp}) \end{aligned} \tag{23}$$

This pre-print refers to the paper presented in 2019 IEEE Milan PowerTech (Milan, 23-27 June 2019), with DOI:10.1109/PTC.2019.8810421

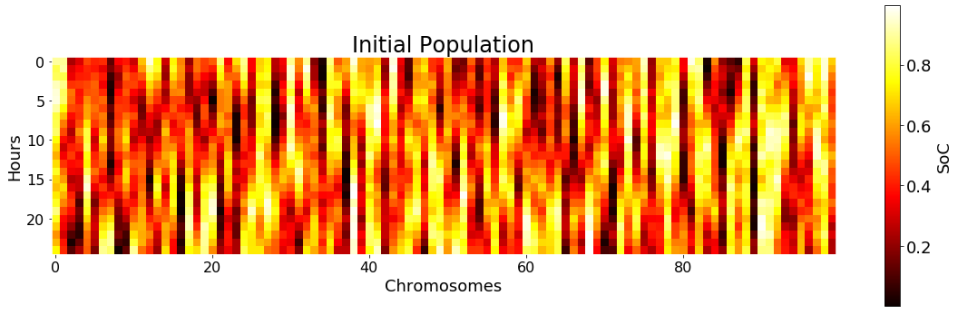

Figure 1: Low $\frac{P_x}{E_x}$ rate BESS, e.g. used for utility energy time shift

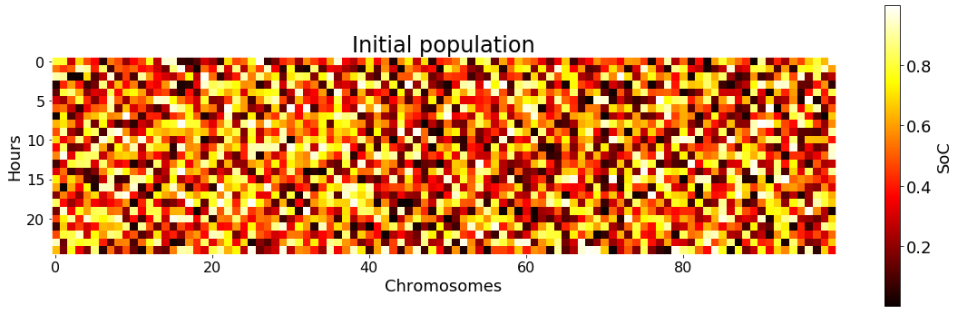

Figure 2: High $\frac{P_x}{E_x}$ rate BESS, e.g. for frequency regulation usage

Figure 3: Uniform distribution of solution within search space.

Again $\mathcal{G}_{n,m} \leftarrow \mathcal{G}_{cr}$ updates the chromosomes subject to crossover.

Mutation for point m is fulfilled by first applying $m-1$ and $m+1$ local constraints as in eq.(24).

$$\begin{aligned} \texttt{lowLim} &= \max(\mathcal{G}_{b,n,i-1}, \mathcal{G}_{b,n,i+1}) - \eta_b^y \cdot \Delta SoC^{max} \\ \texttt{highLim} &= \min(\mathcal{G}_{b,n,i-1}, \mathcal{G}_{b,n,i+1}) + \eta_b^y \cdot \Delta SoC^{max} \end{aligned} \tag{24}$$

The term y is defined in the eq.(refeq:w):

$$y = (\mathcal{G}_{b,n,i+1} - \mathcal{G}_{b,n,i-1}) \tag{25}$$

So, the value of mutation locus can be between filtered limits, as in eq.(26).

$$\mathcal{G} \sim U([\texttt{lowLim}, \texttt{highLim}]) \tag{26}$$

The solutions converge towards to global optima, the Fig. 4 depicts this matter in an intuitive way.

This pre-print refers to the paper presented in 2019 IEEE Milan PowerTech (Milan, 23-27 June 2019), with DOI:10.1109/PTC.2019.8810421

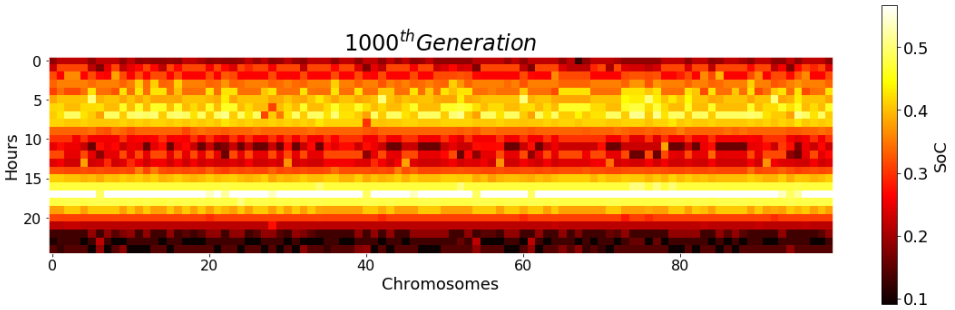

Low $\frac{P_x}{E_x}$ rate BESS, e.g. utility energy time shift

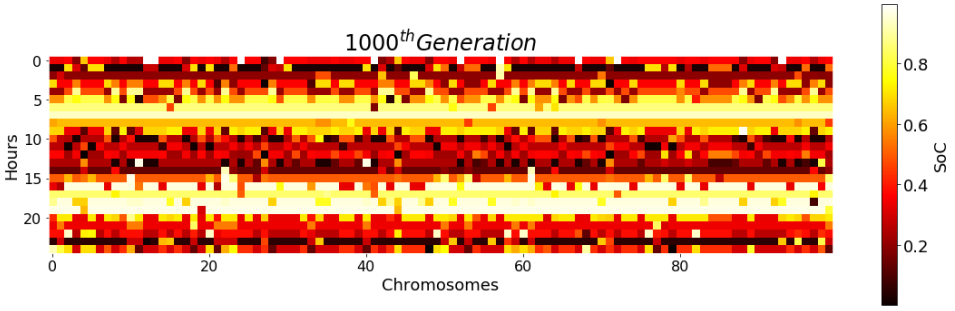

High $\frac{P_x}{E_x}$ rate BESS, e.g. frequency regulation usage

Figure 4: Convergence of the feasible solutions.

5 Case Study and results

As simulation base-ground, a rural Low Voltage (LV) feeder has been modeled which is subject to critical voltage deviation and also unbalance (considerable neutral load) due to high penetration of solar power, long distances from substation and heavy unbalance load distribution. This feeder contains residential and agricultural electricity consumers.

The feeder schema is shown in the Fig. 5. The transformer substation is not depicted in the graph.

For the first part of optimization i.e. sizing and siting BESS, a simulation horizon of one year with one hour granularity is set, consequently load and solar generation profiles contain yearly patterns.

Not all nodes in this system are eligible to BESS installation. There is assumed *a priori* a table of allowed nodes to accommodate BESS in, with determined application of the BESS being installed, e.g. Utility Energy Time Shift, Self RES consumption and Support of Voltage Regulation. The problem in absence of voltage deviation mitigation, in other word $\alpha V_{dev} \ll \beta P_{loss}$ tends to place the BESS close to the distribution substation, but as the weight of V_{dev} increases the search convergence alters.

Once the storage(s) is placed in the best site, one day optimal scheduling

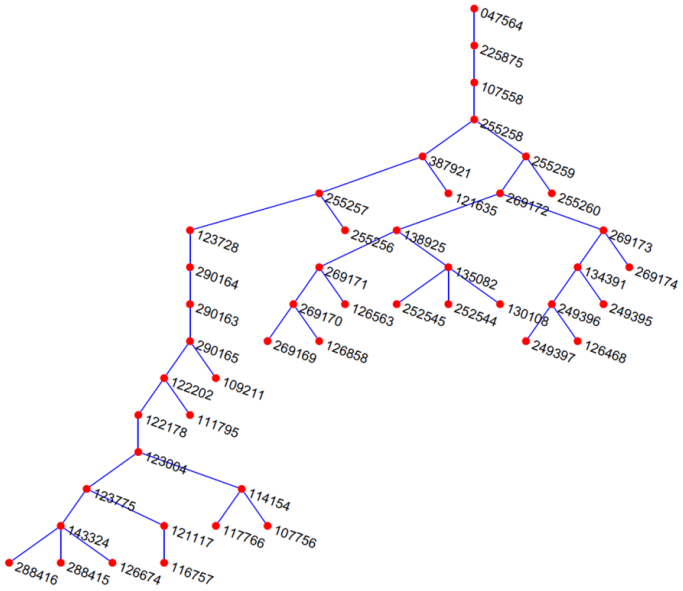

Figure 5: Low voltage rural distribution feeder.

problem with 1 hour resolution is resolved. Objective here is to establish voltage at the connected bus.

Soon, mate pool is being dominated by some of the remote nodes as it can be clearly seen in Fig. 6. From this figure that shows only parents, contains all nodes, various capacity and powers in the initial generation, then gradually nodes with lower impact on voltage correction are excluded.

Fig. 7, instead, reports the selection probability (in PDF) of nodes in optimization progress, where is possible to see that some of the nodes are completely excluded after a while.

6 Conclusion

This paper introduced a hybrid optimization algorithm, designed by considering both the planning phase and the optimanl operation of BESS in the electrical grid. The shown case study investigated the application of the method in a LV network to prove algorithm performance.

This work represents the basis for creating an effective optimization platform that can support storage units deployment in the smart grid framework. The next steps to achieve this purpose are: i) to consider a wider portion of the grid, subject to additional problems, to stress the use of the algorithm and to further improve it; ii) to deeply study the optimization algorithm to set in optimal way all elements; iii) to use more detailed ESS, by also taking into account novel conversion systems such as power-to-gas [21] plants; and

978-1-5386-4722-6/19/$31.00 © 2019 IEEE

This pre-print refers to the paper presented in 2019 IEEE Milan PowerTech (Milan, 23-27 June 2019), with DOI:10.1109/PTC.2019.8810421

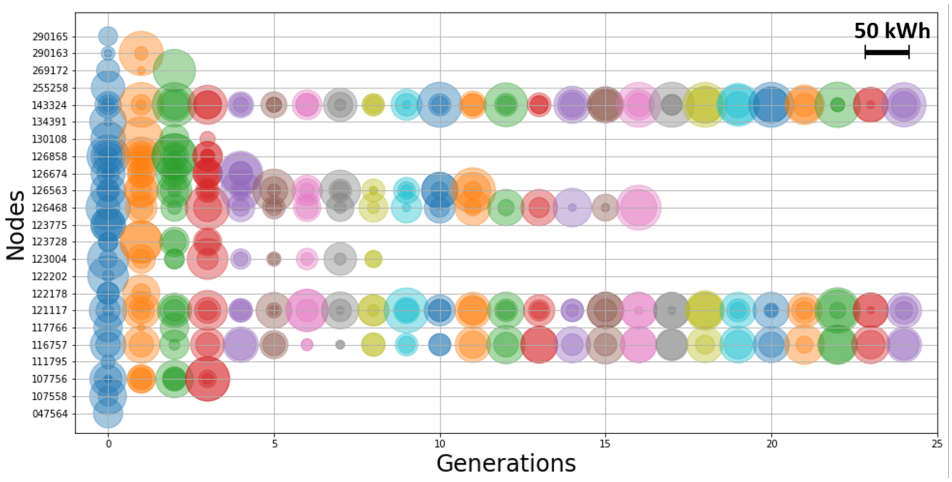

Figure 6: Pool mate of installation nodes and capacity of storages.

iv) to introduce a detailed economical/financial analysis for addressing the optimization by considering economic aspects as well. All the above points will be reached thanks to the proper implementation of the algorithm in a parallel computation framework that will be customized for the system under analysis.

References

[1] O. Ellabban, H. Abu-Rub, and F. Blaabjerg, "Renewable energy resources: Current status, future prospects and their enabling technology," *Renewable and Sustainable Energy Reviews*, vol. 39, pp. 748 – 764, 2014.

[2] H. Zhao, Q. Wu, S. Huang, Q. Guo, H. Sun, and Y. Xue, "Optimal siting and sizing of energy storage system for power systems with large-scale wind power integration," in *2015 IEEE Eindhoven PowerTech*, pp. 1–6, June 2015.

[3] A. Testa, S. D. Caro, R. L. Torre, and T. Scimone, "Optimal design of energy storage systems for stand-alone hybrid wind/pv generators," in *SPEEDAM 2010*, pp. 1291–1296, June 2010.

[4] H. Lu, Y. Li, M. Chen, H. Kim, and S. Serikawa, "Brain intelligence: Go beyond artificial intelligence," *Mobile Networks and Applications*, vol. 23, pp. 368–375, April 2018.

[5] A. Parisio, E. Rikos, and L. Glielmo, "A model predictive control approach to microgrid operation optimization," *IEEE Transactions on Control Systems Technology*, vol. 22, pp. 1813–1827, Sept 2014.

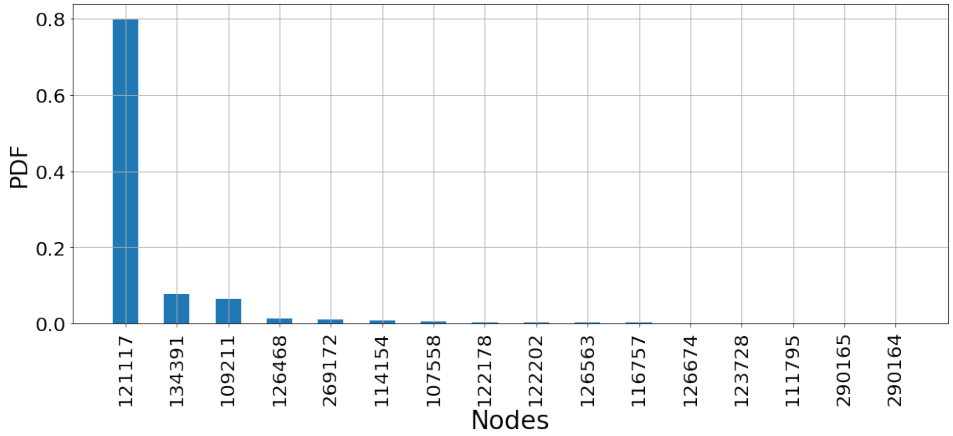

Figure 7: Probability of being selected in entire process.

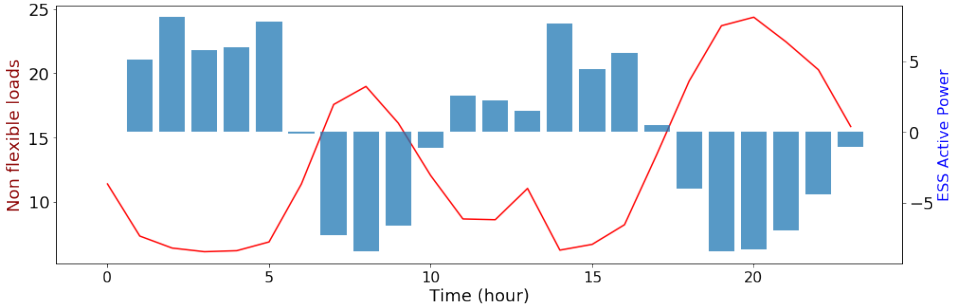

Figure 8: Storage system schedule vs. downstream loads.

[6] R. Tisseur, F. de Bosio, G. Chicco, M. Fantino, and M. Pastorelli, "Optimal scheduling of distributed energy storage systems by means of aco algorithm," in *2016 51st International Universities Power Engineering Conference (UPEC)*, pp. 1–6, Sept 2016.

[7] A. Mazza, G. Chicco, H. Andrei, and M. Rubino, "Determination of the relevant periods for intraday distribution system minimum loss reconfiguration," *International Transactions on Electrical Energy Systems*, vol. 25, pp. 1992–2023, 2015.

[8] P. D. Quevedo, J. Contreras, A. Mazza, G. Chicco, and R. Porumb, "Reliability assessment of microgrids with local and mobile generation, time-dependent profiles, and intraday reconfiguration," *IEEE Transactions on Industry Applications*, vol. 54, pp. 61–72, 2018.

[9] A. Mazza, G. Chicco, and M. Rubino, "Multi-objective distribution system optimization assisted by analytic hierarchy process," in *2012*

IEEE International Energy Conference and Exhibition, ENERGYCON 2012, pp. 1–6, September 2012.

[10] G. Chicco and A. Mazza, "An overview of the probability-based methods for optimal electrical distribution system reconfiguration," in *2013 4th International Symposium on Electrical and Electronics Engineering, ISEEE 2013*, pp. 1–6, October 2013.

[11] T. Lee, "Operating schedule of battery energy storage system in a time-of-use rate industrial user with wind turbine generators: A multipass iteration particle swarm optimization approach," *IEEE Transactions on Energy Conversion*, vol. 22, pp. 774–782, Sept 2007.

[12] A. A. Moghaddam, A. Seifi, T. Niknam, and M. R. A. Pahlavani, "Multi-objective operation management of a renewable mg (micro-grid) with back-up micro-turbine/fuel cell/battery hybrid power source," *Energy*, vol. 36, no. 11, pp. 6490 – 6507, 2011.

[13] Y. A. Katsigiannis, P. S. Georgilakis, and E. S. Karapidakis, "Hybrid simulated annealing–tabu search method for optimal sizing of autonomous power systems with renewables," *IEEE Transactions on Sustainable Energy*, vol. 3, pp. 330–338, July 2012.

[14] O. Babacan, W. Torre, and J. Kleissl, "Optimal allocation of battery energy storage systems in distribution networks considering high pv penetration," in *2016 IEEE Power and Energy Society General Meeting (PESGM)*, pp. 1–5, July 2016.

[15] S. U. Agamah and L. Ekonomou, "Energy storage system scheduling for peak demand reduction using evolutionary combinatorial optimisation," *Sustainable Energy Technologies and Assessments*, vol. 23, pp. 73 – 82, 2017.

[16] Y. Yoon and Y.-H. Kim, "Charge scheduling of an energy storage system under time-of-use pricing and a demand charge," *The Scientific World Journal*, vol. 2014, p. 9, 2014.

[17] Y. Yang, W. Zhang, J. Jiang, M. Huang, and L. Niu, "Optimal scheduling of a battery energy storage system with electric vehicles' auxiliary for a distribution network with renewable energy integration," *Energies*, vol. 8, no. 10, pp. 10718–10735, 2015.

[18] A. Chehouri, R. Younes, J. Perron, and A. Ilinca, "A constraint-handling technique for genetic algorithms using a violation factor," *Journal of Computer Science*, vol. 12, no. 10, pp. 350–362, 2015.

[19] B. Mayoh, E. Tyugu, and J. Penjam, *Constraint Programming*. Springer Science and Business Media, 2013.

This pre-print refers to the paper presented in 2019 IEEE Milan PowerTech (Milan, 23-27 June 2019), with DOI:10.1109/PTC.2019.8810421

[20] B. Battke, T. S. Schmidt, D. Grosspietsch, and V. H. Hoffmann, "A review and probabilistic model of lifecycle costs of stationary batteries in multiple applications," *Renewable and Sustainable Energy Reviews*, vol. 25, pp. 240–250, 2013.

[21] A. Mazza, E. Bompard, and G. Chicco, "Applications of power to gas technologies in emerging electrical systems," *Renewable and Sustainable Energy Reviews*, vol. 92, pp. 794–806, 2018.